

# Proceedings of the Institution of Mechanical Engineers, Part J: Journal of Engineering Tribology

<http://pij.sagepub.com/>

---

## **Stiffness and damping characteristics of lubricated ball bearings considering the surface roughness effect. Part 1: Theoretical formulation**

M Sarangi, B C Majumdar and A S Sekhar

*Proceedings of the Institution of Mechanical Engineers, Part J: Journal of Engineering Tribology* 2004 218: 529

DOI: 10.1243/1350650042794716

The online version of this article can be found at:  
<http://pij.sagepub.com/content/218/6/529>

---

Published by:



<http://www.sagepublications.com>

On behalf of:



[Institution of Mechanical Engineers](http://www.institutionofmechanicalengineers.org)

Additional services and information for *Proceedings of the Institution of Mechanical Engineers, Part J: Journal of Engineering Tribology* can be found at:

**Email Alerts:** <http://pij.sagepub.com/cgi/alerts>

**Subscriptions:** <http://pij.sagepub.com/subscriptions>

**Reprints:** <http://www.sagepub.com/journalsReprints.nav>

**Permissions:** <http://www.sagepub.com/journalsPermissions.nav>

**Citations:** <http://pij.sagepub.com/content/218/6/529.refs.html>

>> [Version of Record](#) - Jun 1, 2004

[What is This?](#)

# Stiffness and damping characteristics of lubricated ball bearings considering the surface roughness effect.

## Part 1: theoretical formulation

M Sarangi, B C Majumdar\* and A S Sekhar

Department of Mechanical Engineering, Indian Institute of Technology, Kharagpur, West Bengal, India

**Abstract:** The stiffness and damping characteristics of isothermal, elasto-hydrodynamically lubricated point contact problems are evaluated numerically considering the surface roughness effect and variation in viscosity with pressure. A set of equations under steady-state and dynamic conditions is derived from the classical Reynolds equation using the linear perturbation method. The elasticity equation and steady-state Reynolds equation are solved simultaneously using the finite difference method with the successive over-relaxation scheme, whereas the dynamic pressures are found after solving the set of perturbed equations using the previously obtained steady-state pressures. The load capacity is obtained from the steady-state pressure distribution. The stiffness and damping coefficients of the contact are determined using the dynamic pressures. Then the overall stiffness and damping matrices of the ball bearing are obtained from the load distribution, coordinate transformation, and compatibility relations.

**Keywords:** ball bearing, damping, elasto-hydrodynamic lubrication, load distribution, rotor-bearing systems, stiffness, surface roughness

### NOTATION

$a, b$	semimajor and semiminor axes respectively of the contact envelope	$\bar{h}, \bar{h}$	film thickness, $\bar{h} = h/R_x$
$c$	inner ring clearance of the bearing	$h_c$	central film thickness
$C, \bar{C}$	damping of a single lubricated contact, $\bar{C} = CU/(E'R_x r)$	$h_T$	average film thickness
$C^b, K^b$	damping and stiffness respectively of a single ball	$\bar{h}_0, \bar{q}_0, \phi_x^0, \phi_y^0$	corresponding steady-state values
$C_i, C_o, K_i, K_o$	inner race contact damping, outer race contact damping, inner race stiffness, and outer race stiffness respectively of each ball	$\Delta h$	perturbation parameter, change in film thickness
$C_b, K_b$	overall damping and stiffness matrices respectively of the bearing	$k$	elliptical parameter = $a/b$
$d$	diameter of the ball = $2r$	$K, \bar{K}$	stiffness of a single lubricated contact, $\bar{K} = K/(E'R_x)$
$d_e$	pitch diameter of the ball bearing = $2r_e$	<b>M, D, K, F</b>	global assembled mass, damping, stiffness and force matrices respectively of the rotor-bearing system
$E'$	combined Young's modulus	$N$	coordinate transformation vector
$E_a, E_b$	Young's moduli of two ellipsoids	$p, \bar{p}$	hydrodynamic pressure, $\bar{p} = p/E'$
$f$	influence coefficient	$\bar{p}_h, \bar{p}_h$	perturbed pressures
$G$	material properties parameter = $\alpha E'$	$P_d$	bearing radial clearance
		$q, \bar{q}$	modified pressure, $\bar{q} = q/E'$
		$\bar{q}_h, \bar{q}_h$	perturbed modified pressures
		$\bar{r}$	geometrical parameter = $r/R_x$
		$r_{ax}, r_{bx}, r_{ay}, r_{by}$	radii of two ellipsoids $a$ and $b$ under contact along the $x$ and $y$ axes respectively
		$r_i, r_o$	inner race and outer race radii respectively
		$R$	equivalent combined contact radius of two ellipsoids, $1/R = 1/R_x + 1/R_y$

The MS was received on 12 January 2004 and was accepted after revision for publication on 26 August 2004.

\* Corresponding author: Department of Mechanical Engineering, Indian Institute of Technology, Kharagpur, West Bengal 721302, India. Email: majum@mech.iitkgp.ernet.in

$R_x, R_y$	equivalent contact radii along the $x$ and $y$ axes respectively
$t$	time
$U, \bar{U}$	combined velocity = $U_a + U_b$ and $\eta_0 U / (E' R_x)$ respectively
$U_a, U_b$	surface velocities of two mating ellipsoids
$\mathbf{u}$	global displacement vector
$V, V_c$	combined elastic deformation and central elastic deformation respectively, $\bar{V} = V/R_x$
$W_i, \bar{W}_i$	load capacity of each ball contact on the race, $\bar{W}_i = W_i / (E' R_x^2)$
$W_x$	total load-carrying capacity of the bearing
$x, y, \bar{x}, \bar{y}$	referred coordinate axes = $x/R_x$ and $y/R_x$ respectively
$\alpha$	pressure–viscosity coefficient of the lubricant
$\beta$	ball contact angle with the race
$\gamma$	surface pattern parameter
$\delta$	elastic deformation
$\varepsilon$	combined local roughness
$\zeta, \mathfrak{S}$	Hertz contact elliptical integrals
$\eta, \eta_0$	absolute viscosity of the lubricant and absolute viscosity of the lubricant in the ambient condition respectively
$A$	hydrodynamic roughness parameter
$\nu_a, \nu_b$	Poisson's ratios of two ellipsoids
$\sigma$	combined standard deviation of roughness
$\tau$	non-dimensional time = $\omega_p t$
$\phi_x, \phi_y, \phi_s$	flow factors
$\varphi, \varphi_1$	load-sharing angle of bearing
$\omega$	angular frequency
$\omega_p$	whirl frequency
$\Omega$	whirl ratio, equal to the ball speed to the ball vibration frequency in the race = $\omega_p / \omega$
$\bar{\bullet}$	non-dimensional parameter

## 1 INTRODUCTION

Ball bearings, known as antifriction bearings, cover a major part of industrial applications. Relative ball motion between the journal and housing plays a key role in supporting load. Friction is reduced due to the rolling action of balls and races. In practice, lubricant is fed into the contact zone of the balls to reduce the friction further. As the load is supported by a relatively small contact area, the pressure developed in the area is high, causing elastic deformation of the contact surfaces.

The elastic deformation and film thickness are sometimes of the same order of magnitude. Hence the elastic deformation must be considered in the theory of hydrodynamic lubrication. Therefore, it is known as elastohydrodynamic lubrication (EHL).

Calculation of the stiffness of ball bearings is performed by treating the contact as dry for simplicity, and damping is almost neglected. The damping characteristic has a substantial influence on the stability of a system. The work presented here is an attempt to evaluate the stiffness and damping characteristics of ball bearings under EHL. The effect of the surface roughness has also been taken into consideration.

Up to the mid-1970s, elliptical contacts in ball bearings were treated as circular contacts or equivalent line contacts to avoid computational time and cost. However, subsequently the availability of faster computers enabled researchers to work on actual elliptical contacts. Hamrock and Dowson [1] presented a comprehensive range of numerical solutions for fully flooded point contacts in which the influence of the ellipticity ratio was considered. The empirical expressions presented in their work are widely used in the design and analysis of machine elements presenting elliptical, lubricated conjunctions. The fluid film thickness in the contact zone becomes few tens of microns to support the load, which is of same order as that of surface roughness. This consideration has attracted the attention of researchers. Patir and Cheng [2] presented the formulation for the average Reynolds equation in terms of pressure and shear flow factors with an assumed Gaussian roughness distribution. The flow factors were presented in the form of simple empirical relations with directional roughness patterns. This roughness model was used by Majumdar and Hamrock [3] for line contact problems, where the average film gap height is obtained analytically. A full numerical solution for partial EHL in elliptical contacts was given by Zhu and Cheng [4] using the same roughness model.

Now the theory of EHL is well understood. However, fewer attempts are being made to study the dynamic characteristics of elastohydrodynamically lubricated contacts, which include the calculation of stiffness and damping. Attempts have been made to investigate damping in ball bearing contacts with relatively simpler experimental models. Zeillinger *et al.* [5] presented experimental work on the calculation of damping coefficients of a ball bearing and subsequently followed the theoretical work of Dietl [6]. In this theoretical study, an elliptical elastohydrodynamically lubricated contact was converted to an equivalent line contact considering the major axis of the ellipse, and the mixed-lubrication stiffness and damping coefficients are evaluated. A relatively high axial load was applied, which allows the assumption of equal load distribution of each ball in the race. This high load in the contact zone may lead to boundary lubrication. Measurement

and theoretical estimation of damping coefficients and related rotor dynamics behaviour have been given in references [7] to [13].

In this paper, the theoretical formulation of the stiffness and damping coefficients of a fully lubricated ball bearing is presented considering the surface roughness. Static and dynamic hydrodynamic pressure equations are derived using a linearized first-order perturbation technique. Overall equivalent bearing stiffness and damping directional matrices are obtained from static load distribution and individual ball contact stiffness and damping, which can be used directly in the finite element method (FEM) analysis of the rotor-bearing system.

**2 THEORY**

**2.1 Elastic deformation**

The two ellipsoids shown in Fig. 1 make a contact at a single point under the unloaded condition and this is called the ‘point’ contact. Geometrical parameters are summarized as follows.

Curvatures in the *x* and *y* directions are defined as

$$\frac{1}{R_x} = \frac{1}{r_{ax}} + \frac{1}{r_{bx}}, \quad \frac{1}{R_y} = \frac{1}{r_{ay}} + \frac{1}{r_{by}}$$

For the ball inner race contact,

$$R_x = \frac{d(d_e - d \cos \beta)}{2d_e}, \quad R_y = \frac{r_i d}{2r_i - d}$$

and, for the ball outer race contact,

$$R_x = \frac{d(d_e + d \cos \beta)}{2d_e}, \quad R_y = \frac{r_o d}{2r_o - d}$$

The point contact spreads to form an elliptical contact due to deformation of the mating surfaces under a normal load. This contact envelope is defined by the elliptical parameter  $k = a/b$ , where *a* and *b* are the semimajor and semiminor axes respectively. The combined elastic deformation of two surfaces can be represented by

$$V(x, y) = \frac{2}{\pi E'} \iint \frac{p(x', y') dx' dy'}{[(x - x')^2 + (y - y')^2]^{1/2}} \tag{1}$$

where

$$E' = \frac{2}{(1 - \nu_a^2)/E_a + (1 - \nu_b^2)/E_b}$$

The integral equation (1) can be solved numerically taking the uniform pressure over an elemental area of  $2d' \times 2b'$  and following a flexibility method of solution

[14] to give

$$V_i = \frac{2}{\pi E'} \sum_{j=1}^n p_j f_{ij} \quad \text{for } i, j = 1, 2, \dots, n \tag{2}$$

where *n* is the total number of elements,  $p_j$  is the distributed pressure over segment *j*, and  $f_{ij}$  is the influence coefficient representing the deflection of segment *i* because of uniform pressure over *j*, given by

$$\begin{aligned} f_{ij} = & (x + b') \ln \left[ \frac{(y + a') + \sqrt{(y + a')^2 + (x + b')^2}}{(y - a') + \sqrt{(y - a')^2 + (x + b')^2}} \right] \\ & + (y + a') \ln \left[ \frac{(x + b') + \sqrt{(y + a')^2 + (x + b')^2}}{(x - b') + \sqrt{(y + a')^2 + (x - b')^2}} \right] \\ & + (x - b') \ln \left[ \frac{(y - a') + \sqrt{(y - a')^2 + (x - b')^2}}{(y + a') + \sqrt{(y + a')^2 + (x - b')^2}} \right] \\ & + (y - a') \ln \left[ \frac{(x - b') + \sqrt{(y - a')^2 + (x - b')^2}}{(x + b') + \sqrt{(y - a')^2 + (x + b')^2}} \right] \end{aligned}$$

**2.2 Hydrodynamic equation**

The hydrodynamic pressure and the mean film thickness are obtained from the numerical solution of the hydrodynamic equation. The governing hydrodynamic equation for rough surfaces can be written as [2]

$$\begin{aligned} \frac{\partial}{\partial x} \left( \phi_x \frac{h^3}{12\eta} \frac{\partial p}{\partial x} \right) + \frac{\partial}{\partial y} \left( \phi_y \frac{h^3}{12\eta} \frac{\partial p}{\partial y} \right) \\ = \frac{U_a + U_b}{2} \frac{\partial h_T}{\partial x} + \frac{U_a - U_b}{2} \sigma \frac{\partial \phi_s}{\partial x} + \frac{\partial h_T}{\partial t} \end{aligned} \tag{3}$$

with film thickness

$$h = h_c - V_c + \frac{x^2}{2R_x} + \frac{y^2}{2R_y} + V$$

where

- $\phi_x, \phi_y$  = pressure flow factors
- $\phi_s$  = shear flow factor
- $\sigma$  = combined standard deviation of rough surfaces
- $h_T$  = average gap height

$h_T$  is given by

$$h_T = \int_{-h}^{\infty} (h + \varepsilon) f(\varepsilon) d\varepsilon$$

where  $f(\varepsilon) = [1/(\sigma\sqrt{2\pi})]e^{-\varepsilon^2/2\sigma^2}$  is the probability density function of combined roughness  $\varepsilon$ . After performing

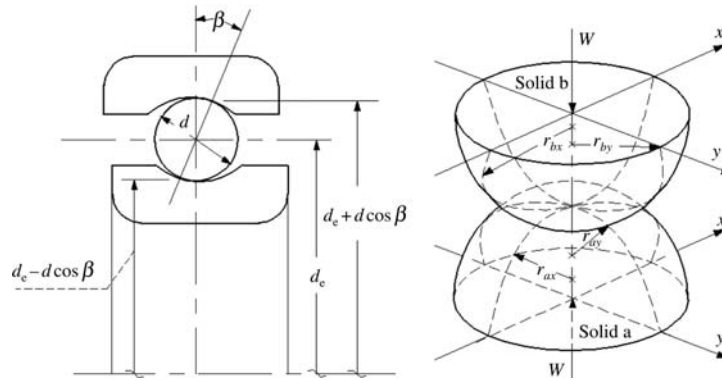


Fig. 1 Geometry of ball bearing and contacting elastic solids

integration and differentiating  $h_T$  with respect to  $x$  or  $t$ ,

$$\frac{\partial h_T}{\partial(x, t)} = \frac{1}{2} \left[ 1 + \operatorname{erf} \left( \frac{h}{\sqrt{2}\sigma} \right) \right] \frac{\partial h}{\partial(x, t)} \quad (4)$$

where

$$\operatorname{erf}(x) = \frac{2}{\sqrt{\pi}} \int_0^x e^{-t^2} dt$$

The expressions for the flow factors can be found in reference [2] and are

$$\phi_x = \begin{cases} 1 - c_1 e^{-g(h/\sigma)} & \text{for } \gamma \leq 1 \\ 1 + c_1 \left( \frac{h}{\sigma} \right)^{-g} & \text{for } \gamma > 1 \end{cases} \quad (5)$$

and

$$\phi_x \left( \frac{h}{\sigma}, \gamma \right) = \phi_y \left( \frac{h}{\sigma}, \frac{1}{\gamma} \right)$$

where  $c_1$  and  $g$  are constants given in Table 1.  $\gamma$  is defined as the ratio of the lengths at which autocorrelation functions of the  $x$  and  $y$  profiles reduce to 50 per cent of the initial values. This can be thought of as the length-to-width ratio of a representative asperity. As per the definition, transverse, isotropic, and longitudinal roughness patterns correspond to  $\gamma < 1$ ,  $\gamma = 1$ , and  $\gamma > 1$  respectively.

Table 1 Constants used in equation (5) for different values of  $\gamma$  [2]

$\gamma$	$c_1$	$g$
$\frac{1}{9}$	1.480	0.42
$\frac{1}{6}$	1.380	0.42
$\frac{1}{3}$	1.180	0.42
1	0.900	0.56
3	0.225	1.50
6	0.520	1.50
9	0.870	1.50

Depending on the type of lubricant, a suitable viscosity variation function can be assumed. For a piezoviscous lubricant, the exponential pressure viscosity relationship is adopted [15] as

$$\eta = \eta_0 e^{\alpha p} \quad (6)$$

Although this relation is approximate, its use makes the modified differential equation (8) linear. However, for a more accurate prediction the relationship given by Roelands [16] can be used. The introduction of the latter relationship makes the differential equation non-linear, which is difficult to handle.

Then pressure can be represented with viscosity variation as

$$q = \frac{1 - e^{-\alpha p}}{\alpha} \quad (7)$$

Making use of equations (3) to (7) and considering pure rolling, the hydrodynamic governing equation can be written in non-dimensional form as

$$\begin{aligned} \frac{\partial}{\partial \bar{x}} \left( \phi_x \bar{h}^3 \frac{\partial \bar{q}}{\partial \bar{x}} \right) + \frac{\partial}{\partial \bar{y}} \left( \phi_y \bar{h}^3 \frac{\partial \bar{q}}{\partial \bar{y}} \right) \\ = 6\bar{U} \left[ 1 + \operatorname{erf} \left( \frac{\Lambda}{\sqrt{2}} \frac{\bar{h}}{\bar{h}_c} \right) \right] \frac{\partial \bar{h}}{\partial \bar{x}} \\ + \frac{6\bar{U}\Omega}{\bar{r}} \left[ 1 + \operatorname{erf} \left( \frac{\Lambda}{\sqrt{2}} \frac{\bar{h}}{\bar{h}_c} \right) \right] \frac{\partial \bar{h}}{\partial \tau} \end{aligned} \quad (8)$$

with film thickness

$$\bar{h} = \bar{h}_c - \bar{V}_c + \frac{\bar{x}^2}{2} + \frac{\bar{y}^2}{2(R_y/R_x)} + \bar{V}$$

where  $\Lambda = h_c/\sigma$  quantifies the severity of roughness. It can be seen from the expressions for  $\phi_x$  and  $h_T$  that, when  $\Lambda$  approaches a large value,  $\phi_x$  approaches 1 and  $\partial h_T/\partial x$  approaches  $\partial h/\partial x$ . Then equation (8) becomes the classical two-dimensional Reynolds equation as applicable for smooth surfaces. Generally  $\Lambda$  varies from 1 for a rough surface to 6 for a smooth surface. The present theory considers only the hydrodynamic

load-supporting ability of a partial elastohydrodynamically lubricated contact. The surface roughness which influences the flow pattern in the contact region gives a pressure distribution different from that of a smooth surface contact. For any small value of  $\Lambda$  (say less than 0.5) the load-supporting ability due to asperity contact will be predominant. The present method does not consider this aspect. The solution of equation (8) with appropriate boundary conditions will give the pressure distribution and film thickness in the contact zone. To find the stiffness and damping of this lubricated contact, a linearized first-order perturbation method is employed as applicable to small displacements. Then the dynamic film thickness and pressure can be expressed as

$$\begin{aligned} h &= h_0 + \Delta h \\ q &= q_0 + q_h \Delta h + q_{\dot{h}} \Delta \dot{h} \end{aligned} \tag{9}$$

where

$$q_h = \frac{\partial q}{\partial h}, \quad q_{\dot{h}} = \frac{\partial q}{\partial \dot{h}}$$

Substituting equation (9) into equation (8), neglecting the second-order terms and collecting the zeroth- and the first-order terms for  $\Delta h$  and  $\Delta \dot{h}$ , the resulting set of equations

$$\frac{\partial}{\partial \bar{x}} \left( \phi_x^0 \bar{h}_0^3 \frac{\partial \bar{q}_0}{\partial \bar{x}} \right) + \frac{\partial}{\partial \bar{y}} \left( \phi_y^0 \bar{h}_0^3 \frac{\partial \bar{q}_0}{\partial \bar{y}} \right) = 6\bar{U} \left[ 1 + \operatorname{erf} \left( \frac{\Lambda}{\sqrt{2}} \frac{\bar{h}_0}{\bar{h}_c} \right) \right] \frac{\partial \bar{h}_0}{\partial \bar{x}} \tag{10}$$

$$\begin{aligned} &\phi_x^0 \bar{h}_0^3 \frac{\partial^2 \bar{q}_h}{\partial \bar{x}^2} + \left( 3\phi_x^0 \bar{h}_0^2 \frac{\partial \bar{h}_0}{\partial \bar{x}} + \bar{h}_0^3 \frac{\partial \phi_x^0}{\partial \bar{x}} \right) \frac{\partial \bar{q}_h}{\partial \bar{x}} + \left( 3\phi_x^0 \bar{h}_0^2 + \bar{h}_0^3 \Delta \phi_x \right) \frac{\partial^2 \bar{q}_0}{\partial \bar{x}^2} + \left( 6\phi_x^0 \bar{h}_0 + 3\bar{h}_0^2 \Delta \phi_x \right) \frac{\partial \bar{q}_0}{\partial \bar{x}} \frac{\partial \bar{h}_0}{\partial \bar{x}} \\ &+ \left[ 3\bar{h}_0^2 \frac{\partial \phi_x^0}{\partial \bar{x}} + \bar{h}_0^3 \frac{\partial (\Delta \phi_x)}{\partial \bar{x}} \right] \frac{\partial \bar{q}_0}{\partial \bar{x}} + \phi_y^0 \bar{h}_0^3 \frac{\partial^2 \bar{q}_h}{\partial \bar{y}^2} + \left( 3\phi_y^0 \bar{h}_0^2 \frac{\partial \bar{h}_0}{\partial \bar{y}} + \bar{h}_0^3 \frac{\partial \phi_y^0}{\partial \bar{y}} \right) \frac{\partial \bar{q}_h}{\partial \bar{y}} + \left( 3\phi_y^0 \bar{h}_0^2 + \bar{h}_0^3 \Delta \phi_y \right) \frac{\partial^2 \bar{q}_0}{\partial \bar{y}^2} \\ &+ \left( 6\phi_y^0 \bar{h}_0 + 3\bar{h}_0^2 \Delta \phi_y \right) \frac{\partial \bar{q}_0}{\partial \bar{y}} \frac{\partial \bar{h}_0}{\partial \bar{y}} + \left[ 3\bar{h}_0^2 \frac{\partial \phi_y^0}{\partial \bar{y}} + \bar{h}_0^3 \frac{\partial (\Delta \phi_y)}{\partial \bar{y}} \right] \frac{\partial \bar{q}_0}{\partial \bar{y}} = 6\bar{U} \Delta \operatorname{erf} \left( \frac{\bar{h}_0}{\bar{x}} \right) \end{aligned} \tag{11}$$

$$\begin{aligned} &\phi_x^0 \bar{h}_0^3 \frac{\partial^2 \bar{q}_{\dot{h}}}{\partial \bar{x}^2} + \left( \bar{h}_0^3 \frac{\partial \phi_x^0}{\partial \bar{x}} + 3\phi_x^0 \bar{h}_0^2 \frac{\partial \bar{h}_0}{\partial \bar{x}} \right) \frac{\partial \bar{q}_{\dot{h}}}{\partial \bar{x}} + \phi_y^0 \bar{h}_0^3 \frac{\partial^2 \bar{q}_{\dot{h}}}{\partial \bar{y}^2} + \left( \bar{h}_0^3 \frac{\partial \phi_y^0}{\partial \bar{y}} + 3\phi_y^0 \bar{h}_0^2 \frac{\partial \bar{h}_0}{\partial \bar{y}} \right) \frac{\partial \bar{q}_{\dot{h}}}{\partial \bar{y}} \\ &= \frac{6\bar{U}\Omega}{\bar{r}} \left[ 1 + \operatorname{erf} \left( \frac{\Lambda}{\sqrt{2}} \frac{\bar{h}_0}{\bar{h}_c} \right) \right] \end{aligned} \tag{12}$$

is found. In the derivation of equations (10) to (12), the variation in  $\phi_x$  and erf functions with film thickness are expressed using Taylor's series according to

$$\phi_x(h_0 + \Delta h) = \phi_x^0 + \Delta \phi_x$$

where  $\phi_x^0 = \phi_x(h_0)$  and

$$\Delta \phi_x = \begin{cases} c_1 g \frac{\Lambda}{\bar{h}_c} e^{-g(\Lambda \bar{h}_0 / \bar{h}_c)} & \text{for } \gamma \leq 1 \\ -c_1 g \frac{\Lambda}{\bar{h}_c} \left( \Lambda \frac{\bar{h}_0}{\bar{h}_c} \right)^{-(g+1)} & \text{for } \gamma > 1 \end{cases}$$

and

$$\Delta \phi_x \left( \Lambda \frac{\bar{h}_0}{\bar{h}_c}, \gamma \right) = \Delta \phi_y \left( \Lambda \frac{\bar{h}_0}{\bar{h}_c}, \frac{1}{\gamma} \right)$$

For the error function erf

$$\operatorname{erf} \left( \frac{\Lambda}{\sqrt{2}} \frac{\bar{h}_0 + \Delta h}{\bar{h}_c} \right) = \operatorname{erf} \left( \frac{\Lambda}{\sqrt{2}} \frac{\bar{h}_0}{\bar{h}_c} \right) + \Delta \operatorname{erf}$$

where

$$\Delta \operatorname{erf} = \frac{2}{\sqrt{\pi}} \left( \frac{\Lambda}{\sqrt{2} \bar{h}_c} \right) e^{-(\Lambda \bar{h}_0 / \sqrt{2} \bar{h}_c)^2}$$

### 3 SOLUTION

#### 3.1 Steady-state solution

The steady-state pressure distribution is obtained with simultaneous solution of equations (2) and (10) and film thickness in equation (8) satisfying the boundary conditions as used in reference [17] and using finite-difference method with successive over-relaxation scheme [18]. The numerical instabilities in the solution due to high load-carrying capacity and high speed can be avoided with the help of introduced relaxation

factors. Sometimes an alternative method of solution such as adaptive meshing or the multi-grid method may overcome this difficulty. Now

$$\bar{q}_{\text{new}} = \bar{q}_{\text{old}} + \operatorname{orf} q (\bar{q}_{\text{new}} - \bar{q}_{\text{old}}) \quad \text{with } \operatorname{orf} q = 1.2-1.5$$

$$\bar{h}_{\text{new}} = \bar{h}_{\text{old}} \left[ 1 + \operatorname{orf} h \left( \frac{\bar{W}_{\text{inew}} - \bar{W}_i}{\bar{W}_i} \right) \right] \quad \text{with } \operatorname{orf} h = 0.01-1$$

$\bar{W}_i$  the total load-carrying capacity of the

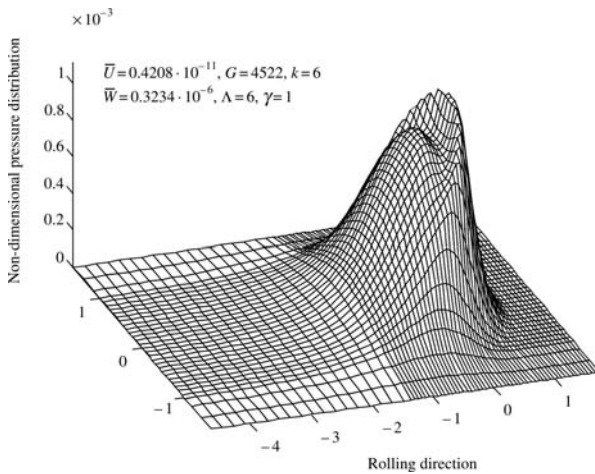


Fig. 2 Steady-state EHL pressure distribution

elastohydrodynamically lubricated contact is

$$\bar{W}_i = \iint_A \bar{p} \, d\bar{x} \, d\bar{y}$$

where

$$\bar{p} = -\frac{\ln(1 - G\bar{q})}{G}$$

Figure 2 shows the non-dimensional pressure distribution as obtained under steady-state solution. The pressure distribution pattern is similar to that of previous work [17] and the non-dimensional minimum film thickness ( $0.11878 \times 10^{-4}$ ) obtained from the present work is close to that in the empirical relation ( $0.12072 \times 10^{-4}$ ) of Hamrock and Dowson [17]. The maximum pressure developed is 0.3023 GPa for the data given in Fig. 2 with the use of 69 mesh points in the rolling direction and 33 mesh points in the transverse direction. A finer mesh is used in the contact region. Obviously with a higher applied load the peak pressure will be more. In the present study the maximum peak pressure obtained is 0.3872 GPa under some operating conditions. For a load that causes a pressure higher than this value, use has to be made of still finer mesh sizes or an alternative method of solution, such as the multi-grid method.

### 3.2 Solution under dynamic conditions

Having obtained the steady-state pressure distribution and film thickness, the pressure distribution under dynamic conditions is obtained from the solution of equations (11) and (12) satisfying appropriate modified boundary conditions using the finite difference method and successive over-relaxation scheme.

### 3.3 Stiffness and damping coefficients

The non-dimensional stiffness and damping coefficients of a single ball contact can be written in terms of dynamic pressure distributions as

$$\bar{K} = \frac{K_1}{E'R_x} = \iint_A \bar{p}_h \, d\bar{x} \, d\bar{y}$$

$$\bar{C} = \frac{C_1 U}{E'R_x r} = \iint_A \bar{p}_h \, d\bar{x} \, d\bar{y}$$

### 3.4 Overall equivalent stiffness and damping matrices of ball bearings

The overall stiffness and damping of a ball bearing are the results of the inner and outer race contact stiffnesses and dampings of individual load-sharing balls, which vary with contact geometry and load-carrying capacity.

A radially loaded ball bearing with radial clearance  $P_d$  is shown in Fig. 3a; the inner ring makes contact under static and no-load conditions. It is noticeable that the clearance at the load line is zero and increases with the angle  $\varphi$ , which can be written as

$$c = \frac{P_d}{2} (1 - \cos \varphi)$$

Now application of the load causes elastic deformation of the balls over the arc  $2\varphi_1$ , and with dynamic conditions there will be a lubricant film to support this external load. Then total interference along the load line ( $\varphi = 0$ ) is given by (see Fig. 3b)

$$\delta^0 = V_c^0 - h_c^0$$

where

$V_c^0$  = combined inner and outer race elastic deformations of the ball along the load line ( $\varphi = 0$ )

$h_c^0$  = combined inner and outer race lubricant film thicknesses in the load line contact ( $\varphi = 0$ )

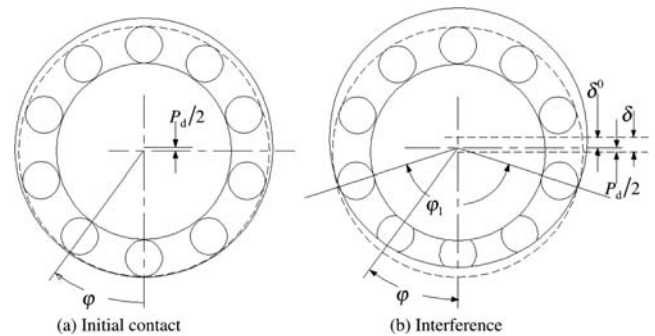


Fig. 3 Radially loaded ball bearing

Interference at any angular position from the load line can be represented in terms of total radial distance of inner ring or shaft from the concentric position  $\delta$  according to

$$\delta_\varphi = \delta \cos \varphi - \frac{P_d}{2} \tag{13}$$

where

$$\delta = \delta^0 + \frac{P_d}{2}$$

Using Hertz elastic deformation and the Hamrock–Dowson [17] film thickness empirical relations,

$$\delta_\varphi = K_H W_\varphi^{2/3} - K_{EHL} W_\varphi^{-0.067} \tag{14}$$

where  $K_H$  is the proportionality of load deformation constant from Hertz contact theory and

$$K_{EHL} = 2.69 \bar{U}_i^{0.67} G_i^{0.53} (1 - 0.61 e^{-0.73k_i}) + 2.69 \bar{U}_o^{0.67} G_o^{0.53} (1 - 0.61 e^{-0.73k_o})$$

is the proportionality constant for load and central film thickness [19], and the subscripts i and o correspond to the inner and outer race contacts respectively.

$K_H$  can be found using the empirical relations for elliptical integrals  $\zeta$  and  $\mathfrak{S}$  of Hertz contact given by Brewe and Hamrock [20] according to

$$\zeta = 1.0003 + \frac{0.5968}{R_y/R_x},$$

$$\mathfrak{S} = 1.5277 + 0.6023 \ln \left( \frac{R_y}{R_x} \right)$$

The deformation at the centre of contact is expressed as

$$\delta = \left( \frac{W}{K} \right)^{2/3}$$

where

$$K = \pi k E' \left( \frac{R_\zeta}{4.5 \mathfrak{S}^3} \right)^{1/2}$$

and combining the deformation due to inner and outer race contact

$$\delta = K_H W^{2/3}$$

with

$$K_H = \left( \frac{1}{K_i} \right)^{2/3} + \left( \frac{1}{K_o} \right)^{2/3}$$

Now the total load-carrying capacity of the bearing is

$$W_x = \sum_0^{\varphi_1} W_\varphi \cos \varphi \tag{15}$$

where

$$\varphi_1 = \cos^{-1} \left( \frac{P_d}{2\delta} \right)$$

Equation (15) is for a pure radial load. The radial, axial loads, and moment due to misalignment for a bearing having contact angle  $\beta$  are given by

$$W_x = \sum_0^{\varphi_1} W_\varphi \cos \varphi \cos \beta$$

$$W_a = \sum_0^{\varphi_1} W_\varphi \sin \beta$$

$$M = -r_e \sum_0^{\varphi_1} W_\varphi \cos \varphi \sin \beta$$

Once the radial load is known, the other two components of load,  $W_a$  and  $M$ , can be found. Equations (13) to (15) will be solved using the non-linear least-square method and iteratively with successive over-relaxation on the change in  $\delta$  according to

$$\delta_{\text{new}} = \delta_{\text{old}} \left[ 1 + \text{orfd} \left( \frac{W_{x\text{new}} - W_x}{W_x} \right) \right]$$

with  $\text{orfd} = 0.1-1$

Having obtained the load sharing, the individual equivalent stiffness and damping coefficients of each ball can be calculated as a combination of inner and outer race contact stiffnesses (Fig. 4).

If two linear spring–damper combinations are connected in series as in Fig. 4, the resulting equivalent frequency dependent stiffness and damping can be determined with the help of the complex equation [6]

$$K^b + j\omega C^b = \left( \frac{1}{K_i + j\omega C_i} + \frac{1}{K_o + j\omega C_o} \right)^{-1} \tag{16}$$

where  $\omega$  is the angular frequency, which is generally of the inner race, outer race, cage, or ball pass frequencies or combinations of two or more of these [21]. It is appropriate to take the combination of inner and outer race ball pass frequencies, as they contribute more in dynamics of the system. Replacing a ball with the equivalent spring–damper system (Fig. 4), it may be possible to find the overall stiffness matrix  $\mathbf{K}_b$  and damping matrix  $\mathbf{C}_b$  from the compatibility and

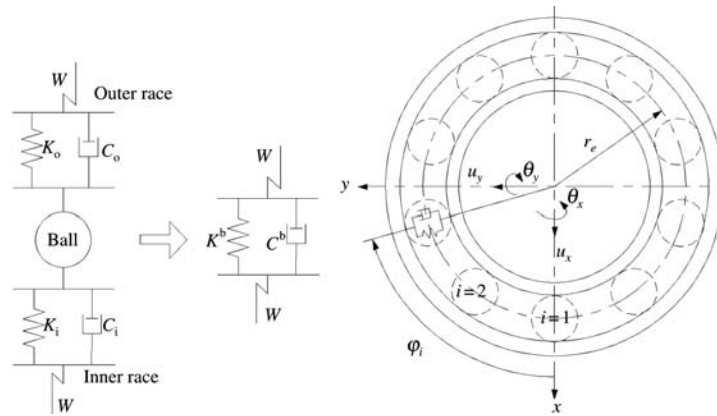


Fig. 4 Equivalent stiffness and damping model of ball bearing

coordinate transformation matrix as

$$\begin{aligned}
 \mathbf{K}_b &= \sum_{i=1}^z K_i^b \mathbf{N}_i^T \mathbf{N}_i \\
 \mathbf{C}_b &= \sum_{i=1}^z C_i^b \mathbf{N}_i^T \mathbf{N}_i
 \end{aligned} \tag{17}$$

where  $z$  is the number of balls under contact (within the arc  $2\varphi_1$ ) and  $N$  is the transformation vector with global displacement vector  $\mathbf{u} = \{u_x, u_y, \theta_x, \theta_y\}^T$ . The displacement along the axial direction is neglected, which is generally not considered for the finite element formulation of rotor systems. Also,

$$\mathbf{N}_i = \begin{Bmatrix} \cos \varphi_i \cos \beta \\ \sin \varphi_i \cos \beta \\ r_e \sin \varphi_i \sin \beta \\ -r_e \cos \varphi_i \sin \beta \end{Bmatrix}^T$$

#### 4 APPLICATION TO ROTOR-BEARING SYSTEMS

The stiffness and damping matrices as formulated in equation (17) can be used in rotor-bearing systems. Characteristic equations are summarized for the case of a rotor-bearing system (Fig. 5) to understand the influence of lubricated ball bearings on the dynamics of rotor systems [22]. The system characteristic equation will be assembled considering individual components using the FEM [23, 24].

##### 4.1 Finite rotor element

A Timoshenko beam element with four degrees of freedom per node is considered [24], whose equation of

motion is given as

$$(\mathbf{M}_R + \mathbf{M}_T)\ddot{\mathbf{u}} + (\mathbf{B} - \Omega\mathbf{G})\dot{\mathbf{u}} + (\mathbf{K}_B - \mathbf{K}_A)\mathbf{u} = \mathbf{F} \tag{18}$$

where

- $\mathbf{M}_R$  = rotational mass matrix
- $\mathbf{M}_T$  = translational mass matrix
- $\mathbf{K}_B$  = bending stiffness matrix of the Timoshenko beam
- $\mathbf{K}_A$  = axial stiffness matrix due to the axial load
- $\mathbf{B}$  = damping matrix
- $\mathbf{G}$  = gyroscopic matrix
- $\mathbf{u} = \{u_x, u_y, \theta_x, \theta_y\}^T$  generalized degrees of freedom
- $\mathbf{F}$  = external excitation force

##### 4.2 Bearing element

Neglecting the mass of bearing, the equation of motion for bearing can be written as

$$\mathbf{C}_b \dot{\mathbf{u}}_b + \mathbf{K}_b \mathbf{u}_b = \mathbf{F}_b \tag{19}$$

where the subscript b corresponds to the bearing degrees of freedom.

##### 4.3 Rigid disc

The disc is assumed to have an effect like a concentrated mass and so it can be characterized solely by kinetic energies. Mass and inertia properties can be concen-

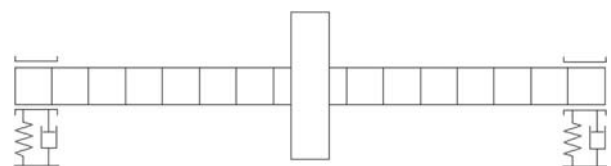


Fig. 5 Rotor-bearing system model

trated on the corresponding node on the shaft [22]. Hence, a disc element with a single node and four degrees of freedom has been used for modelling the disc according to

$$\mathbf{M}_d \ddot{\mathbf{u}}_d - \Omega \mathbf{G}_d \dot{\mathbf{u}}_d = \mathbf{F}_d \quad (20)$$

where  $\mathbf{M}_d$  and  $\mathbf{G}_d$  are the mass and gyroscopic matrices respectively of the disc. The subscript d corresponds to the disc nodal degrees of freedom.

#### 4.4 System equation of motion

After assembling equations (18) to (20), the system equation of motion becomes

$$\mathbf{M}\ddot{\mathbf{u}} + \mathbf{D}\dot{\mathbf{u}} + \mathbf{K}\mathbf{u} = \mathbf{F} \quad (21)$$

where  $\mathbf{M}$  is the global mass matrix of the system and includes the mass matrices of shaft and disc. The matrix  $\mathbf{D}$  includes the damping matrices of shaft and bearings as well as the gyroscopic matrices of shaft and disc. The global stiffness matrix  $\mathbf{K}$  is the contribution of stiffness matrices of shaft and bearings. Equation (20) can be solved using the state-space method in the absence of external excitation for the eigen analysis. The forced vibration characteristics can be studied with inclusion of the external excitation force.

## 5 CONCLUSION

A procedure for the numerical evaluation of the stiffness and damping coefficients of isothermal, elastohydrodynamically lubricated ball bearings for elliptical contacts is outlined. This needs simultaneous solution of the elasticity and hydrodynamic equations as well as the dynamic pressure equations and load distribution. A non-uniform mesh is adopted for numerical solution, which reduces the computational time. An attempt has been made to derive suitable empirical formulae for the calculation of stiffness and damping coefficients of lubricated point contacts using a non-linear least-square curve-fitting technique with different numerically evaluated data presented in the subsequent paper (Part 2). This approach will avoid the necessity of time-consuming numerical calculations. The analysis is applicable to a complete range of fully lubricated ball bearings with relatively moderate load.

## REFERENCES

- 1 Hamrock, B. J., and Dowson, D. Isothermal elastohydrodynamic lubrication of point contacts. Part I: theoretical formulation. *Trans. ASME, J. Lubric. Technol.*, 1976, **98**(2), 223–229.
- 2 Patir, N., and Cheng, H. S. An average flow model for determining effects of three-dimensional roughness on partial hydrodynamic lubrication. *Trans. ASME*, 1978, **100**, 12–17.
- 3 Majumdar, B. C., and Hamrock, B. J. Effect of surface roughness on elastohydrodynamic line contact. *Trans. ASME, J. Lubric. Technol.*, 1982, **104**, 401–408.
- 4 Zhu, D., and Cheng, H. S. Effect of surface roughness on the point contact EHL. *Trans. ASME, J. Tribology*, 1988, **110**, 32–37.
- 5 Zeillinger, R., Springer, H., and Kötttritsch, H. Experimental determination of damping in rolling bearing joints. In Proceedings of the 39th ASME International Gas Turbine and Aeroengine Congress/Users Symposium and Exposition, The Hague, The Netherlands, paper 94-GT-102, 1994 (American Society of Mechanical Engineers, New York).
- 6 Dietl, P. Damping and stiffness characteristics of rolling element bearings, theory and experiments. PhD thesis, Mechanical Engineering, Technical University of Vienna, Vienna, Austria, 1997.
- 7 Elsermans, M., Hongerloot, M., and Snoeye, R. Damping in taper roll bearings. In Proceedings of the 16th Machine Tool Design and Research (MTDR) Conference, 1976, pp. 223–229.
- 8 Wijnant, Y. H. Contact dynamics in the field of elastohydrodynamic lubrication. PhD thesis, University of Twente, The Netherlands, 1998.
- 9 Wijnant, Y. H., and Venner, C. H. Analysis of an EHL circular contact incorporating rolling element vibration. In Proceedings of the 23rd Leeds–Lyon Symposium on Tribology (Eds D. Dowson *et al.*), Leeds, September 1996, 1997, pp. 445–456.
- 10 Wijnant, Y. H., and Venner, C. H. Analysis of an EHL circular contact incorporating rolling element vibration. In Proceedings of the 25th Leeds–Lyon Symposium on Tribology (Eds D. Dowson *et al.*), Leeds, September 1998, 1999, pp. 705–716.
- 11 Wijnant, Y. H., Venner, C. H., Larsson, R., and Eriksson, P. Effect of structural vibration on the film thickness in an EHL circular contact. *Trans. ASME, J. Tribology*, 1999, **121**(2), 259–264.
- 12 Hendrikx, R. T. W. M., Nijen, G. C. V., and Dietl, P. Vibration in household appliances with rolling element bearings. In *Noise and Vibration Engineering*, Proceedings of the 23rd International Symposium on the Strength of Metals and Alloys (ISMA23), 1998 Vol. 3, pp. 1537–1544.
- 13 Wensing, J. A. On the dynamics of ball bearings. PhD thesis, University of Twente, The Netherlands, 1998.
- 14 Hertnett, M. J. The analysis of contact stresses in rolling element bearings. *Trans. ASME, J. Lubric. Technol.*, 1979, **101**, 105–109.
- 15 Barus, C. Isotherms, isopiestic and isometrics relative to viscosity. *Am. J. Sci.*, **45**, 87–96.
- 16 Roelands, C. J. A. *Correlational Aspects of the Viscosity–Temperature–Pressure Relationship of Lubricating Oils*, 1966 (Druk VRB, Groningen).
- 17 Hamrock, B. J., and Dowson, D. *Ball Bearing Lubrication*, 1981 (John Wiley, New York).
- 18 Sarangi, M., and Majumdar, B. C. Development of codes for estimating minimum film thickness and traction for ball bearings lubricated with liquid having low-pressure vis-

- osity coefficients. Report, Indian Institute of Technology, Kharagpur, India, 2003.
- 19 Hamrock, B. J., and Dowson, D.** Isothermal elastohydrodynamic lubrication of point contacts. Part III: fully flooded results. *Trans. ASME, J. Lubric. Technol.*, 1977, **99**, 264–276.
- 20 Brewster, D. E., and Hamrock, B. J.** Simplified solution for elliptical-contact deformation between two elastic solids. *Trans. ASME, J. Lubric. Technol.*, **99**(4), 485–487.
- 21 Goodwin, M. J.** *Dynamics of Rotor–Bearing Systems*, 1989 (Unwin Hyman, London).
- 22 Nelson, H. D., and McVaugh, J. M.** The dynamics of rotor–bearing systems using finite elements. *Trans. ASME, J. Engng Industry*, May 1976, **98**(2), 593–600.
- 23 Nelson, H. D.** A finite rotating shaft element using Timoshenko beam theory. *Trans. ASME, J. Mech. Des.*, 1980, **102**, 793–803.
- 24 Ozguven, H. N., and Ozkan, Z. L.** Whirl speeds and unbalance response of multi bearing rotor using finite elements. *Trans. ASME, J. Vibr., Acoust., Stress Reliability Des.*, 1984, **106**, 72–79.